Hypersonic anomalies and optical properties of $RbTiOAsO_4$ and $KTiOPO_4$ single crystals

Chi-Shun Tu
Department of Physics, Fu-Jen University, Taipei 242, Taiwan, Republic of China

Ram S. Katiyar
Department of Physics, University of Puerto Rico, Rio Piedras, Puerto Rico 00931

V. Hugo Schmidt
Department of Physics, Montana State University, Bozeman, Montana 59717

Ruyan Guo and A. S. Bhalla
Materials Research Laboratory, The Pennsylvania State University, University Park, Pennsylvania 16802

(Received 23 December 1997; revised manuscript received 6 August 1998)

The longitudinal (LA) Brillouin back-scattering spectra along the [001] phonon direction have been measured as a function of temperature for $RbTiOAsO_4$ (RTA) and $KTiOPO_4$ (KTP) single crystals. As temperature increases, the acoustic-phonon frequencies of RTA and KTP show a clear softening (which reaches a turning point at $T_c \sim 800\,^{\circ}C$ for RTA). We conclude that the transitions in RTA and KTP are either weakly first order or of second order. It seems likely that the alkali ions (K^+ or Rb^+) are strongly involved in the soft mode. A broad damping evolution (which attains a maximum at $T_c \sim 800\,^{\circ}C$ in RTA) was observed for both crystals and can be attributed to the dynamic order-parameter fluctuations. The optical transmissions, refractive indices (n_x, n_y, n_z) and the Cauchy equations (for RTA) were obtained as a function of wavelength. The LA[001] sound velocities V_{LA} and elastic constants $C_{33}+(e_{33}^2/\varepsilon_{33}^s)$ were also calculated at room temperature for both crystals. [S0163-1829(99)10501-0]

I. INTRODUCTION

Rubidium titanyl arsenate ($RbTiOAsO_4$) (RTA) and potassium titanyl phosphate ($KTiOPO_4$) (KTP) belong to the family of nonlinear optical crystals with the general formula $M^{1+}TiOX^{5+}O_4$, where $M=\{K,Rb,Tl,Cs\}$ and $X=\{P,As\}$.[1–8] The high damage threshold and broad angular acceptance have made such crystals attractive materials for frequency doubling of Nd-based lasers at $\lambda=1.064$ and 1.32 μm, and for optical parametric oscillators (OPO). In addition, the ion exchange properties also make them one of the best candidates for waveguide applications.

KTP-type crystals have an orthorhombic unit cell (which contains eight formula units) at room temperature and a ferroelectric- (FE) paraelectric (PE) phase transition with a change of symmetry $mm2$ (space group $Pna2$)-mmm ($Pnam$).[8] The crystal framework is a three-dimensional structure made from corner-linked TiO_6 octahedra and PO_4 tetrahedra. Four oxygen ions of the TiO_6 belong to PO_4 tetrahedral groups which link the TiO_6 groups. In our earlier Raman results, a slight softening was exhibited by several LO and TO vibrational modes of RTA and KTP.[1,2] A transition to a higher symmetry structure was evidenced by the disappearance of the A_{1g} (LO) stretching mode of the TiO_6 group near T_c for both RTA and KTP.[1,2] However, there is no typical soft mode observed in the low-frequency modes of the Raman spectra. This motivated us to carry out Brillouin-scattering measurements to look for softening in the acoustic modes.

We report here the temperature-dependent acoustic-phonon spectra and wavelength dependences of optical transmission and refractive indices. The Cauchy equations $[n(\lambda)=A+B/\lambda^2+C/\lambda^4]$ for n_x, n_y and n_z are also obtained for RTA. Direct evidence for acoustic phonon soft modes in both RTA and KTP is presented. In particular, a microscopic mechanism for the phase transition based on a ''point-charge model'' is proposed.

II. EXPERIMENTAL PROCEDURE

Single crystals of $RbTiOAsO_4$ and $KTiOPO_4$ were grown using the tungstate flux method.[1] The crystals were oriented by x-ray diffraction and were cut into rectangular shape having (100), (010), and (001) faces. The surfaces for measurements were well polished to be optically smooth. The Brillouin spectra were obtained from the back-scattering geometry with configuration $z(yu)\bar{z}$. ''u'' means that the collection was not polarization discriminated. Here, y and z correspond to the crystal b and c axes, respectively. The sample was illuminated along [001] with an Innova 90 plus-A3 argon laser with $\lambda=514.5$ nm, so the longitudinal phonons with wave vector along [001] were studied. According to the theoretical calculation for an orthorhombic structure (all classes), there should be no transverse acoustic (TA) mode in the case of backscattering due to weak intensity factor.[9] Scattered light was analyzed by a Burleigh five-pass Fabry-Perot interferometer. In our experiments, the free spectral ranges (FSR) of the Fabry-Perot are determined by measuring the LA phonon shift of fused quartz. The free spectral range was 25.18 GHz for the RTA spectra and 29.05 GHz for the KTP spectra of this paper. To improve the spectral resolution, the Brillouin doublet was adjusted to appear

in the second order with respect to the Rayleigh lines. The laser line half-width (for $\lambda = 514.5$ nm) is about 0.02 GHz determined by the spectrometer. To avoid sample heating, the laser power incident on the samples was kept less than ~120 mW. An optical furnace with maximum temperature near 1000 °C was used with a K-type thermocouple. To determine the accurate positions and half-widths of the Brillouin components, the damped harmonic-oscillator model with the spectral response function,[1]

$$S(\omega) = \frac{\chi_0 \Gamma \omega \omega_0^2}{(\omega^2 - \omega_0^2)^2 + \Gamma^2 \omega^2} \cdot \frac{1}{1 - e^{-\hbar\omega/kT}}, \qquad (1)$$

was used, where ω_0 and $\Gamma (= \Gamma_{obs})$ correspond to the phonon frequency and observed half-width, respectively, χ_0 is the susceptibility constant (in arbitrary units), k is Boltzmann's constant, and T is the absolute temperature. For backscattering, the broadening due to collection optics is negligible.[10] In this case, the natural-phonon half-width Γ_{obs} is given by $\Gamma_{ph} = \Gamma_{obs} - \Gamma_{inst}$.[10] In our experiments, the half-width of the Rayleigh line from fused quartz (which was assumed to have a Gaussian distribution) was taken as the instrumental broadening $\Gamma_{inst} \sim 0.006$ FSR.

For measurements of optical transmission, a *Varian Model Cary* 5E UV-Vis-NIR *Spectrophotometer* (0.2–3.0 μm) and a *Perkin-Elmer 2000 Model* FTIR (2.0–6.0 μm) were used. A *J. A. Woollam Co. Model VB-200 Variable Angle Spectroscopy Ellipsometer* with WVASE32™ analyzing software was utilized for determination of refractive indices. The refractive indices were determined by measuring the change of polarization between incident and reflected beams.

III. RESULTS AND DISCUSSION

Actual temperature-dependent LA[001] phonon spectra of the anti-Stokes Brillouin component are shown in Figs. 1(a) and 1(b) for RTA and KTP, respectively. The solid lines are fits of Eq. (1), from which the frequency shift and half-width Γ_{obs} were obtained. The temperature-dependent phonon frequency exhibits a negative coupling (softening) with increasing temperature for both crystals. Figures 2(a) and 2(b) shows the temperature dependences of the frequency shift and half-width Γ_{ph}. Comparing the half-widths, we notice that the average damping value is stronger in KTP. Also, due to uncertainty of collection angle which can appreciably broaden and distort Brillouin line shape, the half-width data [Figs. 2(a) and 2(b)] show scatter (which is more pronounced in RTA).[10–12] Such an uncertainty can be associated with the temperature-dependent refractive indices and slight misalignment of sample orientation. The phonon frequency reduction (in the measured temperature range) are about 9.3 and 8.8 % for RTA and KTP, respectively.

In order to estimate the effect of coupling, we calculated the bare (uncoupled) phonon frequency $\omega_a(T)$ by fitting the low-temperature measured values. Here, we assume that room temperature is far away from the coupled region since the ferroelectric phase transition occurs at $T \approx 800$ °C for RTA and $T \sim 930$ °C for KTP. The bare phonon frequency is defined as the phonon frequency far from the phase transition. The temperature-dependent $\omega_a(T)$ can be described by the Debye anharmonic approximation;[12]

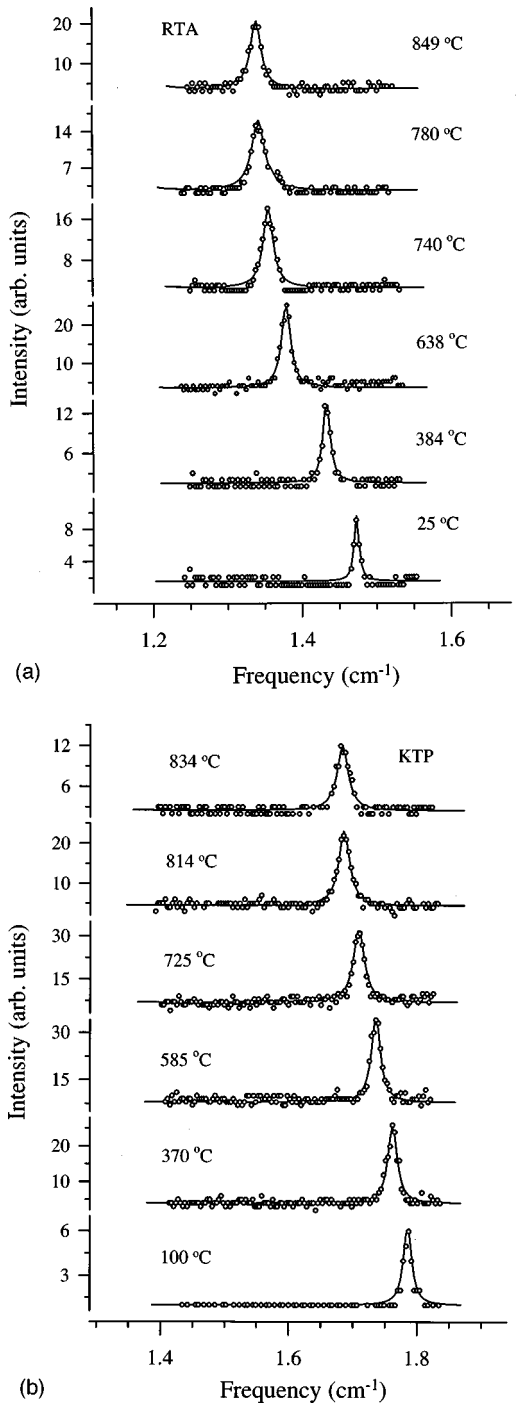

FIG. 1. Anti-Stokes components of the LA[001] Brillouin frequency spectra for (a) RTA and (b) KTP. The solid lines area fits of Eq. (1).

$$\omega_a(T) = \omega_a(0)\left[A\Theta F\left(\frac{\Theta}{T}\right)\right], \qquad (2)$$

where Θ is the Debye temperature, ''A'' represents the amount of anharmonicity and ''F'' is the Debye function for internal energy.[12]

In Figs. 2(a) and 2(b), the dashed lines are the calculations of Eq. (2) with parameters given in Table I. The measured phonon frequency begins to deviate from the bare frequency at $T \sim 500$ °C (for RTA) and $T \sim 650$ °C (for KTP). It implies that the acoustic soft modes begin to set in near $T \sim 500$ °C

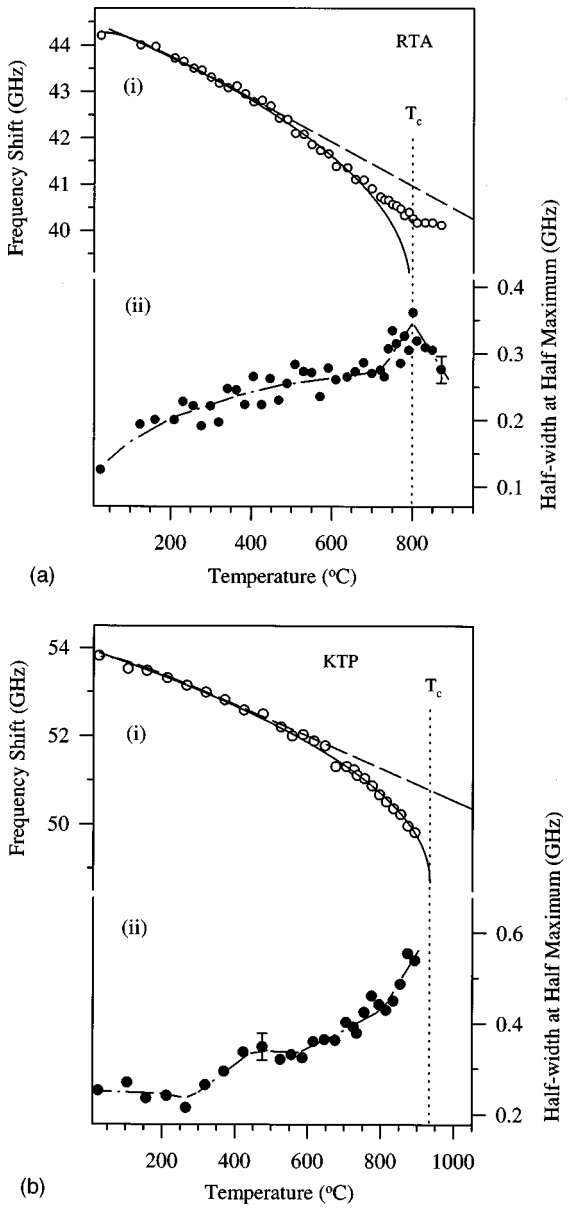

FIG. 2. (i) Brillouin frequency shift (open circles) and (ii) half-width Γ_{ph} (solid circles) vs temperature of the LA[001] phonons for (a) RTA and (b) KTP. The dashed line is the Debye anharmonic calculation with parameters given in Table I. The solid line is a fit of the equation, $\omega = a(T_c - T)^{1/2} + b$, with parameters given in Table II. The dotted lines indicate the ferroelectric phase transitions at $T_c \sim 800$ and $\sim 930\,^{\circ}\mathrm{C}$ for RTA and KTP, respectively. The dot-dashed lines are qualitative estimates of the order-parameter fluctuation contributions.

and $T \sim 650\,^{\circ}\mathrm{C}$ in RTA and KTP, respectively. The frequency reduction (between ~ 500 and $\sim 800\,^{\circ}\mathrm{C}$) in RTA due to the soft mode is about 4.8%. For a typical FE phase transition, the transition temperature occurs where the frequency shift curve has an abrupt change. In RTA, the acoustic-phonon frequency reaches a turning point near 800 °C. Thus, the FE transition temperature of the RTA single crystal is $T_c \sim 800\,^{\circ}\mathrm{C}$. This value is close to the $T_c = 795 \pm 5\,^{\circ}\mathrm{C}$ of $RbTiOPO_4$ (RTP).[5]

Ferroelectric transitions are known to be associated with a soft mode of lattice motion. Lines and Glass point out that if the transition is strongly first order, mode softening may not be detectable.[13] Based on the dielectric and spontaneous birefringence results, a nearly second-order displacive phase transition has been proposed for KTP, RTP ($RbTiOPO_4$) and TTP ($TlTiOPO_4$).[7,8] The solid lines in Figs. 2(a) and 2(b) are the fits using the equation, $\omega = a(T_c - T)^{1/2} + b$, with parameters listed in Table II. We note that a zone-center ($q = 0$) acoustic soft mode in the reduced Brillouin zone of the reciprocal sublattice always has a zero frequency as approaching T_c from the ordered phase, i.e., $T \rightarrow T_c^-$, for a second-order transition.[13] Therefore, the nonzero minimum of frequency shift at T_c implies that the structural instabilities (as $T \rightarrow T_c^+$) in RTA and KTP must be associated with a more complicated mode, or else it implies that the transition is weakly first order.[13] Furthermore, the phonon frequency shift of RTA begins to deviate from the solid line at $T \sim 720\,^{\circ}\mathrm{C}$. It indicates that a hardening mode begins to develop as T approaches T_c^-. Such a phenomenon is stimulated by the structural instability and implies a new structural symmetry to be built for the high-temperature phase ($T > T_c$). As temperature increases, the phonon shift of KTP also shows a rapid softening. However, the Brillouin signal became undetectable above $T \sim 900\,^{\circ}\mathrm{C}$, probably due to rapid oxidization on the KTP sample surface.

The phonon dampings [solid circles in Figs. 2(a) and 2(b)] of both RTA and KTP exhibit a gradual growth from room temperature up to near T_c. Such a slowly rising anomaly reveals that order-parameter fluctuations are the dominant dynamic mechanism. Qualitative estimates of this fluctuation contribution are given by the dot-dashed curves in Figs. 2(a) and 2(b) (with a maximum peak near $T_c \sim 800\,^{\circ}\mathrm{C}$ in RTA). The dynamic fluctuation contribution is a characteristic of a $\eta^2\mu$-type electrostrictive coupling, squared in order parameter and linear in strain.[14]

The ferroelectric nature of the titanyls appears to result in large part from the alkali cations being displaced along the polar axis. In $KTiOPO_4$, in the notation of Ref. 15 which has b instead of the usual choice c for the polar axis, the K^+ ions are displaced by 0.642 Å along the negative b axis from the positions required for a mirror plane at $y/b = 0.5$ which would destroy the polarization. This pseudomirror plane is clearly seen in their Fig. 1 [001] projection. In this figure, the K(1) ion is (from their Table II) at $y/b = 0.312\,01$. Its pseudomirror image partner, seen almost above it in their Fig. 1, is at $y/b = 0.566\,90$ because it is the 2_1 screw-axis

TABLE I. Parameters from the fits of Eq. (2) to room-temperature values of frequency shift.

	$\omega_a(0)$ (GHz)	Θ	A (K^{-1})
RTA	44.28	300	1.08×10^{-4}
KTP	53.80	300	6.80×10^{-5}

TABLE II. Parameters from the fits of equation, $\omega = a(T_c - T)^{1/2} + b$, to measured values of frequency shift.

	a (GHz/°$C^{1/2}$)	b (GHz)	T_c (°C)
RTA	0.204	38.76	794
KTP	0.172	48.70	934

partner of K(2) which from their Table II is at $y/b = 0.066\,90$. The mean y/b position of K(1) and its pseudomirror image ion is $(0.312\,01+0.566\,90)/2 = 0.439\,455$, which is 0.060 545, or 0.642 Å, below the pseudomirror plane at $y/b = 0.5$. On a point-charge model, with charge $+e$ at the K^+ sites, and with eight formula units per orthorhombic unit cell of size $a = 12.814$ Å, $b = 10.616$ Å, and $c = 6.404$ Å, this 0.642 Å displacement would contribute -0.0944 C/m^2 to the spontaneous polarization P_s.

In a similar way, one finds that the other point-charge model contributions to P_s are—0.055 22 C/m^2 from the oxygens (charge $-2e$) not bonded to phosphates, $-0.055\,87$ C/m^2 from PO_4^{-3} ions considered as $-3e$ charges at the phosphorus sites, and $+0.0045$ C/m^2 from those Ti^{4+} ions which are not already on the hypothetical mirror plane. These contributions provide a total spontaneous polarization of $P_s = -0.2010$ C/m^2, and the potassium ions are responsible for nearly half of this amount. Measurements of P_s in these titanyls are hampered by their high electrical conductivity. However, a value of $P_s = 0.144$ C/m^2 has been measured in $CsTiOAsO_4$ (CTA),[16] which is near the magnitude of our calculated value for KTP. The sign of P_s depends on which direction of the polar axis is chosen as positive in the crystal coordinate system.

The rms thermal vibration amplitude for the K^+ ions is 0.24 Å, considerably greater than for the other ions.[15] Accordingly, the transition may result from the thermal amplitude becoming large enough so that the ions assume average positions consistent with conversion of the 2_1 symmetry element to a mirror or glide plane. The symmetry of the high-temperature phase of KTP is not certain. The authors of first x-ray study considered $Pnma$ and $Pn2_1a$ as possible room-temperature structures.[15] They obtained considerably better fit for $Pn2_1a$, but their consideration of $Pnma$ and viewing of their c projection (their Fig. 1) indicate that $Pnam$ (in standard notation) is a liekly possibility for the paraelectric phase.[15] However, Allan *et al.*[17] consider $Pnan$ more likely as the high-temperature point group in their report on a high-pressure x-ray study of KTP. They propose as the transition mechanism ''polyhedral tilting in the TiO_6-PO_4 framework being driven by the softening low-frequency Raman mode near 56 cm^{-1}.'' Kourouklis *et al.*[18] found this mode had a small discontinuity at the phase transition at 5.5 GPa at room temperature, indicating that this pressure-driven transition is weakly first order. This Raman mode has been associated with the K^+ ions.[19]

From our Fig. 2(a), the temperature dependences of the frequency shift and half-width for RTA both exhibit rather weak cusps centered at T_c. The softening in KTP [shown in Fig. 2(b)] has progressed further than it did even at the RTA transition. From the above considerations, we propose that the transitions in RTA and KTP are either weakly first order (as for KTP's pressure-driven transition discussed above) or of second order. It seems likely that the alkali ions, K^+ (or Rb^+) in these two cases, are strongly involved in the soft mode.

The optical percent transmissions (0.2–6.0 μm) of RTA and KTP measured in the [001] direction are shown in Fig. 3. As compared to RTA, KTP has a higher optical transmission between ~0.35 and 2.8 μm, but its transmission shows a strong overtone absorption at ~3.0–3.5 μm and begins to drop at ~4.3 (~5.3 μm in RTA). The sharp absorption bands at 2803 nm (for KTP) and 2862 nm (for RTA) most likely represent the O–H stretching band and indicate that H^+ has been incorporated into the structure.[20,21] The absorption beginning at ~4200 nm (in KTP) and ~5000 nm (in RTA) correspond to the molecular (PO_4, AsO_4, and TiO_6) bands.[21] The broad absorption regions at ~3000–3500 nm (for KTP) and ~3800–4300 nm (for RTA) are attributed to the overtones of molecular (PO_4, AsO_4, and TiO_6) absorption bands.[20] As a result, the orthophosphate absorption at ~4.3 and ~3.5 μm in KTP could severely limit the oscillator output power. In contrast, RTA has a broader infrared transparency (~0.35–5.3 μm) and exhibits no strong overtone absorption. This makes the RTA crystal a potential candidate for nonlinear optical applications.

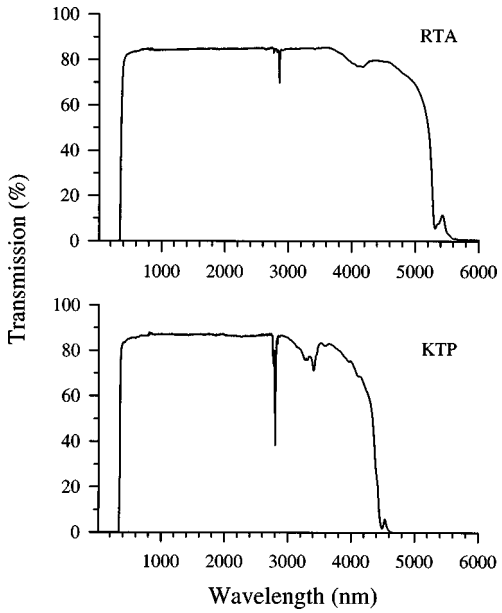

FIG. 3. Optical percent transmissions of RTA and KTP observed in the [001] direction.

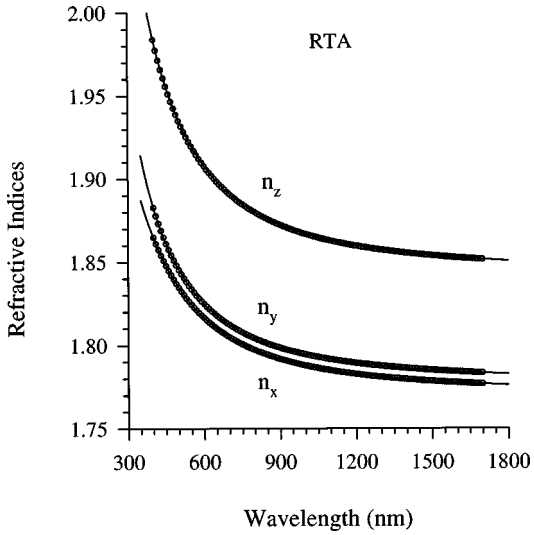

FIG. 4. Refractive indices (n_x, n_y, n_z) of RTA. Solid lines are fits to the Cauchy equations with parameters given in Eq. (3).

TABLE III. Refractive indices and birefringences ($n_z - n_x$) of RTA for four wavelengths.

λ (μm)	n_x	n_y	n_z	$n_z - n_x$
0.532	1.8278	1.8374	1.9247	0.0969
0.66	1.8089	1.8165	1.8967	0.0878
1.064	1.7859	1.7925	1.8641	0.0782
1.32	1.7806	1.7872	1.8568	0.0762

Figure 4 shows the wavelength-dependent refractive indices (n_x, n_y, and n_z) of RTA measured at room temperature. The solid lines are the fits of Cauchy equations with parameters listed below:

$$n_z(\lambda) = 1.8432 + \frac{0.02379}{\lambda^2} - \frac{0.0002041}{\lambda^4},$$

$$n_y(\lambda) = 1.7773 + \frac{0.01722}{\lambda^2} - \frac{0.0000567}{\lambda^4}, \qquad (3)$$

$$n_x(\lambda) = 1.7706 + \frac{0.01765}{\lambda^2} - \frac{0.0004138}{\lambda^4}.$$

The unit of wavelength (λ) in Eq. (3) is μm. We summarize the refractive indices of four wavelengths (which could be used for frequency doubling of Nd-based lasers at $\lambda = 1.064$ and 1.342 μm) in Table III. The intrinsic optical birefringence of RTA decreases with increasing wavelength. The birefringence ($n_z - n_x = 0.0782$ at 1.064 μm) of RTA is smaller than that for KTP ($n_z - n_x = 0.0921$ at 1.064 μm).[22] This reduction of birefringence makes RTA an ideal material for frequency doubling at higher fundamental wavelengths such as 1.32 μm for the Nd:YAG laser line.

Brillouin scattering is a powerful tool to determine related acoustic parameters such as elastic constants. The associated theories and calculations of connected parameters can be found in Ref. 10. At room temperature, the sample density is $\sim 4.02 \times 10^3$ kg/m^3 for RTA and $\sim 3.03 \times 10^3$ kg/m^3 for KTP.[15,23] In our experiments, the measured phonon is along the [001] direction ($\bar{q} \| [001]$). By solving the secular equation (3) of Ref. 10, one obtains

$$\rho V_{\mathrm{LA}}^2 = \rho \left(\frac{\lambda_o \Delta \nu_{\mathrm{LA}}}{2n \sin(\theta/2)} \right)^2 = C_{33} + \frac{e_{33}^2}{\varepsilon_{33}^s}, \qquad (4)$$

where λ_0 is the wavelength of the incident light in vacuum, θ is the scattering angle inside the crystal ($\theta \sim 180°$ in this report), $\Delta \nu_{\mathrm{LA}}$ is the longitudinal phonon frequency shift, e_{ij} is the piezoelectric stress constant, and ε_{jj}^s is the static permittivity at constant strain. The related calculated values for both RTA and KTP are given in Table IV. One can expect that the smaller sound velocity and elastic constant in RTA are mainly due to the heavier atomic masses of rubidium and arsenite. Here, the refractive index n_z of KTP was taken from Ref. 22.

TABLE IV. Refractive indices n_z ($\lambda = 5.145$ nm), LA[001] sound velocities V_{LA} and elastic constants $C_{33} + (e_{33}^2/\varepsilon_{33}^s)$ measured at room temperature.

	n_z	V_{LA} (m/s)	$C_{33} + (e_{33}^2/\varepsilon_{33}^s)(10^{11}$ N/m$^2)$
RTA	1.930	5888	1.39
KTP	1.895	7305	1.62

IV. CONCLUSIONS

A main feature of the LA[001] acoustic-phonon spectra of RTA and KTP is that a temperature-dependent character has been observed in both the phonon frequency and half-width Γ_{ph}. As temperature increases, the acoustic-phonon soft modes appear near 500 (in RTA) and 650 °C (in KTP). In RTA, the phonon frequency reaches a nonzero turning point (associated with a maximum damping peak) at $T_c \sim 800$ °C which is the transition temperature. We conclude that the transitions in RTA and KTP are either weakly first order or of second order. It seems likely that the alkali ions, K^+ (or Rb^+) in these two cases, are strongly involved in the soft mode. From the half-width temperature dependences, we conclude that order parameter fluctuations are the dominant contribution for the broad damping evolutions in both RTA and KTP. A quadratic $\eta^2 \mu$-type electrostrictive coupling is considered to be the main contribution to the acoustic phonon softening in both crystals. The data of optical percent transmission shows that RTA has a broader infrared transparency ($\sim$0.35–5.3 μm) and exhibits no strong overtone absorption as compared to KTP. In addition, refractive indices (n_x, n_y, n_z) and the Cauchy equations of RTA were obtained as a function of wavelength. The LA[001] sound velocities V_{LA} and elastic constants $C_{33} + (e_{33}^2/\varepsilon_{33}^s)$ were also calculated at room temperature for both RTA and KTP.

ACKNOWLEDGMENTS

The authors express sincere thanks to Y.-L. Yeh, Z.-Q. Xue, G.-W. Lee, and P.-F. Chen for their help on experiments. This work was supported by NSC87-2112-M-030-001 and NSF Grant No. DMR-9520251.

[1] C.-S. Tu, R R. Guo, R. Tao, R. S. Katiyar, R. Guo, and A. S. Bhalla, J. Appl. Phys. **79**, 3235 (1996).

[2] A. R. Guo, C.-S. Tu, R. Tao, R. S. Katiyar, R. Guo, and A. S. Bhalla, Ferroelectrics **188**, 143 (1996).

[3] L. K. Cheng, L.-T. Cheng, J. D. Bierlein, and F. C. Zumsteg, Appl. Phys. Lett. **62**, 346 (1993).

[4] L. T. Cheng, L. K. Cheng, J. D. Bierlein, and F. C. Zumsteg, Appl. Phys. Lett. **63**, 2618 (1993).

[5] G. Marnier, B. Boulanger, and B. Menaert, J. Phys.: Condens. Matter **1**, 5509 (1989).

[6] L. K. Cheng, L. T. Cheng, and J. D. Bierlein, Appl. Phys. Lett. **64**, 1321 (1994).

[7] V. K. Yanovskii, V. I. Voronkova, A. P. Leonov, and S. Y. Stefanovich, Sov. Phys. Solid State **27**, 1508 (1985).

[8] Y. V. Shaldin and R. Poprawski, Ferroelectrics **106**, 399 (1990).

[9] R. Vacher and L. Boyer, Phys. Rev. B **6**, 639 (1972).

[10] C.-S. Tu, V. H. Schmidt, and I. G. Siny, J. Appl. Phys. **78**, 5665 (1995).
[11] H. G. Danielmeyer, J. Acoust. Soc. Am. **47**, (Part 2), 151 (1970).
[12] C.-S. Tu and V. H. Schmidt, Phys. Rev. B **50**, 16 167 (1994).
[13] M. E. Lines and A. M. Glass, *Principles and Applications of Ferroelectrics and Related Materials* (Oxford, London, 1977).
[14] W. Rehwald, Adv. Phys. **22**, 721 (1973); C.-S. Tu, Ph.D. thesis, Montana State University, 1994.
[15] I. Tordjman, R. Masse, and J. C. Guitel, Z. Kristallogr. **139**, S103 (1974).
[16] G. M. Loiacono, D. N. Loiacono, and R. A. Stolzenberger, J. Cryst. Growth **131**, 323 (1993).
[17] D. R. Allan, J. S. Loveday, R. J. Nelmes, and P. A. Thomas, J. Phys.: Condens. Matter **4**, 2747 (1992).
[18] G. A. Kourouklis, A. Jayaraman, and A. A. Ballman, Solid State Commun. **62**, 379 (1987).
[19] R. V. Pisarev, R. Farhi, P. Moch, and V. I. Voronkova, J. Phys.: Condens. Matter **2**, 7555 (1990).
[20] D. L. Pavia, G. M. Lampmann, and G. S. Kriz, *Introduction to Spectroscopy*, 2nd ed. (Saunders College Publishing, New York, 1996).
[21] F. C. Zumsteg, J. D. Bierlein, and T. E. Gier, J. Appl. Phys. **47**, 4980 (1976).
[22] Y. F. Tso, C. E. Huang, B. Q. Hu, R. C. Eckardt, Y. X. Fan, R. L. Byer, and R. S. Feigelson, Appl. Opt. **26**, 2390 (1987).
[23] P. A. Thomas, S. C. Mayo, and B. E. Watts, Acta Crystallogr., Sect. B: Struct. Sci. **48**, 401 (1992).